Materials and Design 35 (2012) 120–125

Contents lists available at SciVerse ScienceDirect

Materials and Design

journal homepage: www.elsevier.com/locate/matdes

Effects of processing parameters on microstructure and mechanical property of selective laser melted Ti6Al4V

Bo Song *, Shujuan Dong, Baicheng Zhang, Hanlin Liao, Christian Coddet

LERMPS-Université de Technologie de Belfort – Montbéliard, Site de Sévenan, 90010 Belfort Cedex, France

ARTICLE INFO

Article history:
Received 10 August 2011
Accepted 23 September 2011
Available online 29 September 2011

Keywords:
C. Lasers
E. Mechanical
F. Microstructure

ABSTRACT

Selective laser melting, as a facile method, was successfully used in this paper to manufacture perfect Ti6Al4V parts. Based on a series of single tracks, the processing windows were firstly proposed, corresponding to different melting mechanisms. And selective laser melted Ti6Al4V parts using various parameters within the processing map were investigated in terms of microstructure, roughness, densification and microhardness. It was found that the microstructure, roughness, densification and microhardness of Ti6Al4V parts were a strong function of processing parameters. An excellent Ti6Al4V part with the high microhardness and the smooth surface can be manufactured by selective laser melting using preferable laser power 110 W and scanning speed 0.4 m/s, corresponding to continuous melting mechanism. The density is so high that it can be comparable to that of bulk Ti6Al4V alloy.

1. Introduction

Titanium alloys have been widely applied for load-bearing orthopedic implants in the physiological environment due to their attractive properties, such as high corrosion resistance and excellently soft and hard tissue biocompatibility [1–4]. Among titanium alloys, Ti6Al4V is the most favorable since its first introduction in the early 1950s. However, due to the intrinsic property of pre-alloyed Ti6Al4V, it is difficult to elaborate parts using Ti6Al4V feedstock.

The existing studies on manufacturing technology for Ti6Al4V focused on the traditional processing method, casting. This process not only needs to prepare a complex mold but also has the oxidation problem of Ti6Al4V, phase transitions, decomposition and grain growth, due to the high-temperature holding for a long time.

Selective laser melting (SLM), as one of the rapid prototyping techniques, was proposed in the present paper to manufacture Ti6Al4V parts. SLM represents an evolution of selective laser sintering (SLS) process when the complete melting of powder occurs rather than sintering or partial melting [5]. After noticeable improvements in recent years, this processing technique appears which can transform metallic and alloy powders directly into dense parts, in contrast to selective laser sintering (SLS) where post-processing is needed to obtain fully dense parts [6]. During the SLM process, once a powder layer has been scanned, the building platform moves down one step (typically between 30 and 100 μm), and the next powder layer is placed upon the previous one by means of a powder feeder. After all layers have been deposited, the rest powder which was not scanned can be removed and the produced part can be taken out of the machine [7,8]. These advantages promote its potential for material processing and rapid manufacturing applications. Recent research efforts have also demonstrated that SLM, due to its flexibility in feedstock and shapes, has a promising potential for the net-shape production of complex-shaped, high-performance composites parts. SLM processes of Al–Si–Mg/SiC, stainless steel/hydroxyapatite, 663 copper alloy, Fe–Ni–Cr and TiC/Ti5Si3 powder have been reported [9–13]. Thus, SLM, as a facile method, was tentatively used to melt Ti6Al4V powder.

In this paper, the importance of the processing parameters in striving to obtain fully dense Ti6Al4V parts by selective laser melting has been demonstrated. The effects of processing parameters on the microstructure, roughness, densification and microhardness were carried out.

2. Experimental procedure

2.1. Powder used

The Ti6Al4V powder used as feedstock was prepared in the laboratory by gas atomization and thus has a spherical shape. The distribution size is homogeneous as shown in Fig. 1a. Spherical or near-spherical particles generally result in close packing, thereby leading to a more efficient densification during SLM process. Fig. 1b shows an essential lognormal distribution with a particle size of 10.62 μm (d10), 18.35 μm (d50) and 31.46 μm (d90).

* Corresponding author. Tel.: +33 3 84583564; fax: +33 3 84583286.
E-mail address: bo.song@utbm.fr (B. Song).

0261-3069/$ - see front matter © 2011 Elsevier Ltd. All rights reserved.
doi:10.1016/j.matdes.2011.09.051

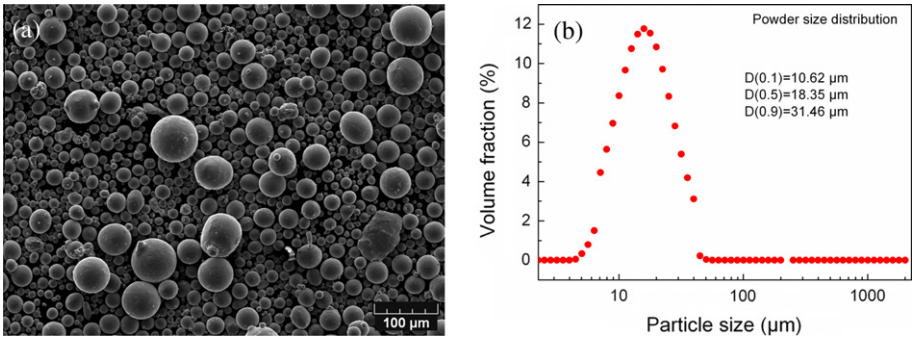

Fig. 1. (a) SEM morphology and (b) size distribution of Ti6Al4V powder.

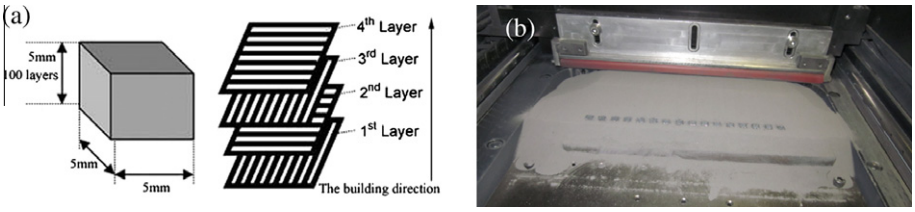

Fig. 2. (a) Layer cross-hatching technique and (b) photographs showing real-time selective laser melting process.

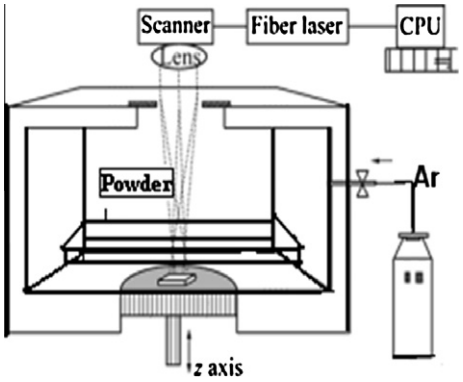

Fig. 3. Schematic diagram of selective laser melting machine.

2.2. Selective laser melting process

Stainless steel plates of 25 mm × 10 mm × 5 mm dimensions were used as stacking platform. Before being installed, this platform was grit-blasted with alumina. In order to identify a range of suitable parameters for manufacturing Ti6Al4V alloy, a series of single tracks with length 10 mm were firstly melted. And then a set of 5 mm long, 5 mm wide and 5 mm thick specimens were produced using various parameters as illustrated in Fig. 2.

The laser source of the SLM machine used is a YLR-100-SM single mode CW Ytterbium fiber laser (1064–1100 nm). The diameter of laser beam is adjustable between 34 μm and 75 μm and the maximum power is 120 W. The maximum laser scanning speed is v = 3 m/s. The working chamber provides a closed environment which is filled with Argon as a protective gas to maintain the pressure of oxygen below (0.8%), where the temperature of stacking platform can be adjusted and fixed at 100 °C. SLM was performed in the following ranges: laser beam 34 μm, laser power from 70 and 120 W, laser scanning speed 0.05–1.6 m/s, scan line spacing 40 μm and powder layer thickness 50 μm. The SLM machine was schematically shown in Fig. 3.

2.3. Characterization

The top-surface microstructure of melted Ti6Al4V parts was characterized using a scanning electron microscope. The cross-sectional microstructure of Ti6Al4V parts was examined by optical microscope (OM). The density was estimated using Archimedean method. The Vickers hardness of polished parts was measured under 300 g load with load time 15 s. Each mean hardness value is obtained from 20 measurements. The surface roughness of Ti6Al4V parts was obtained with a Taylor–Hobson Surtronic 3P profilometer.

3. Results and discussion

3.1. Mechanisms of powder melting

As well known, the densification level and the attendant microstructure of selective laser melted Ti6Al4V parts depend strongly on

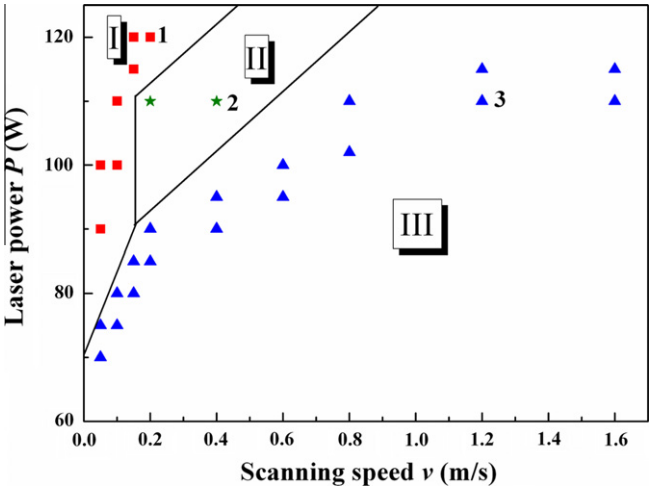

Fig. 4. Mechanisms of single tracks for selective laser melted Ti6Al4V (zone I-melting with cracks, zone II-continuous melting, zone III-partial melting) versus laser power and scanning speed.

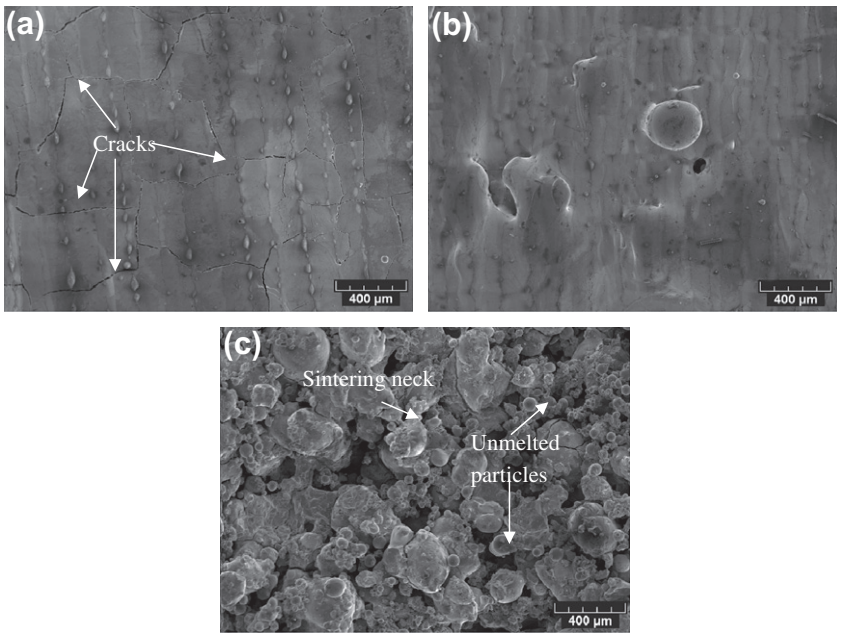

Fig. 5. SEM images showing typical top-surface morphologies of selective laser melted samples with selected parameters in different processing windows: (a) 120 W, 0.2 m/s (point 1, within zone I), (b) 110 W, 0.4 m/s (point 2, within zone II), and (c) 110 W, 1.2 m/s (point 3, within zone III).

the operating temperature of the melting system, which is mainly controlled by two main parameters, i.e., laser power and scanning speed. Thus, 27 single tracks were firstly melted in the present paper in order to clarify the melting mechanism of Ti6Al4V powder

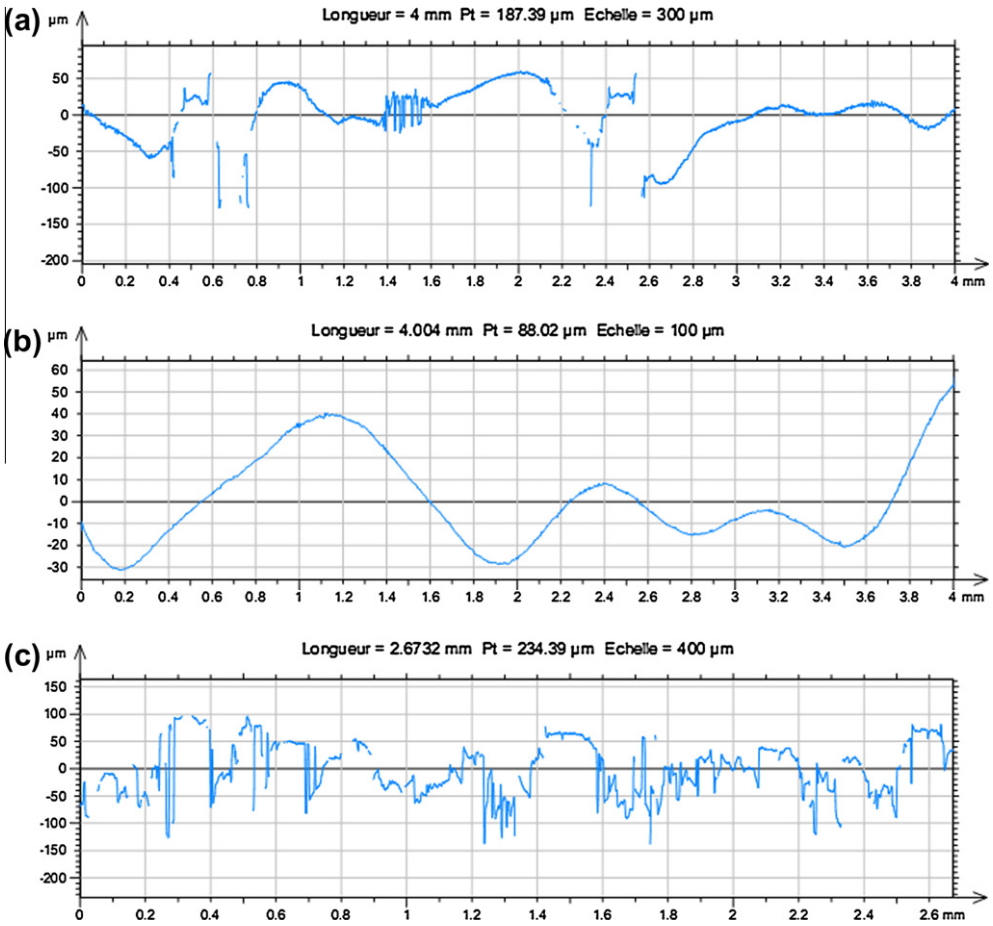

Fig. 6. Surface roughness of selective laser melted Ti6Al4V parts corresponding to different processing windows: (a) 120 W, 0.2 m/s (point 1, within zone I), (b) 110 W, 0.4 m/s (point 2, within zone II), and (c) 110 W, 1.2 m/s (point 3, within zone III).

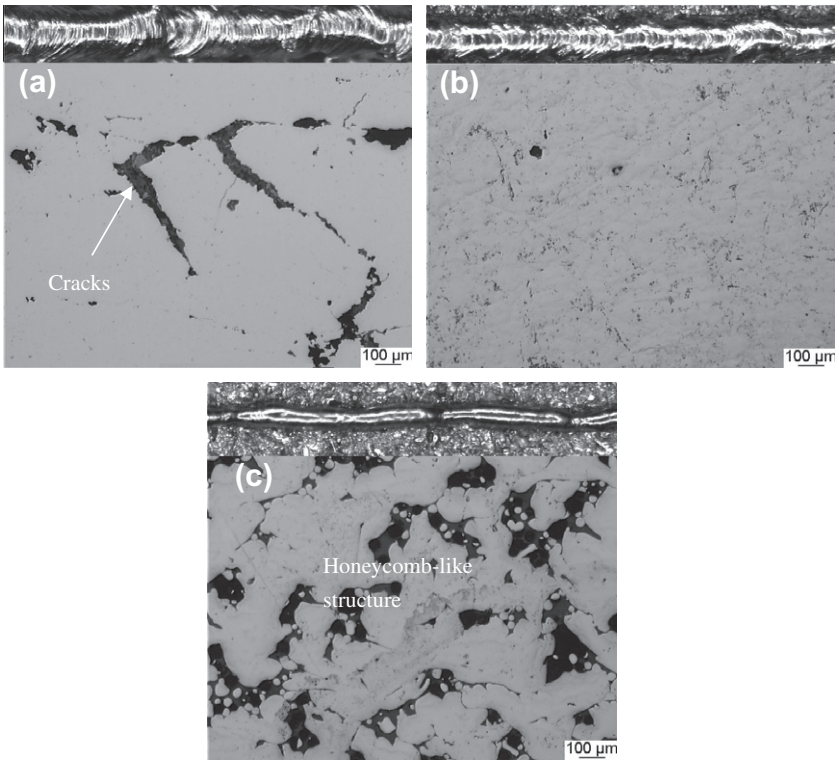

Fig. 7. OM micrographs of single tracks (top) and cross-sectional Ti6Al4V parts (bottom) produced by different processing parameters: (a) 120 W, 0.2 m/s, (b) 110 W, 0.4 m/s, and (c) 110 W, 1.2 m/s.

Table 1
Density of selective laser melted Ti6Al4V parts with different melting mechanism.

Melting mechanism	Melting with cracks	Continuous melting	Partial melting
Process window	Zone I	Zone II	Zone III
Density (g/cm^3)	3.87	4.13	2.91

and to later manufacture a perfect part. A processing map was then defined, based on the series of single tracks, which were indicated by different symbols in Fig. 4. Over the entire range of laser powers and scanning speeds, three processing windows could be summarized, corresponding to three different melting mechanisms:

(I) *Melting with cracks*. This is a high energy input zone. At a high laser power combined with a relatively low scanning speed, the single Ti6Al4V track could be completely melted and even broke up duo to the excessive shrinkage and the high residual stresses, producing many visible cracks.

(II) *Continuous melting*. The energy input was so comfortable that continuous single tracks were obtained by means of the complete melting of Ti6Al4V powders.

(III) *Partial melting*. The insufficient energy input could not induce significant melting of Ti6Al4V powders. This will inevitably induce a laminated structure formed by Ti6Al4V powders.

Once this processing map was defined, the three processing windows could be used to choose the suitable conditions under which a perfect part can be successfully produced.

The characteristic top-surface morphologies of Ti6Al4V parts produced by selective laser melting according to the described windows are provided in Fig. 5. Selective laser melting using parameters within zone I (point 1) yielded a split surface containing many cracks, despite producing a relatively dense surface. However, these cracks are harmful for the performance of selective laser melted Ti6Al4V. As to point 2 within zone II, a relatively smooth and dense melted surface was obtained. And the metallurgical bonding took place. This fact implies that all the single tracks have a better metallurgical bonding with each other. In fact, this metallurgical bonding is a complex process, including multiple heat and mass transfer and in some instances chemical reactions as reported in other literatures [14–18]. In case of point 3 within zone III, it can be recognized that there exist many unmelted particles and balling phenomenon can be found. This balling phenomenon can be explained by the melting instability during the selective laser melting process. It is particularly pronounced in the case of insufficient energy input zone. On one hand, the lower laser energy results in a decrease of the diameter of cylindrical tracks and even leads to a significant transverse shrinkage distortion, namely, thin and dis-

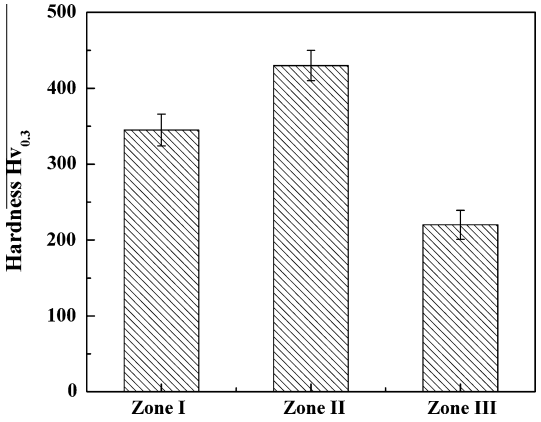

Fig. 8. Microhardness of selective laser melted Ti6Al4V parts.

continuous tracks as the results (top in Fig. 7c) in the following sections. On the other hand, a number of small-sized liquid droplets, in turn, tend to splash from the surface of those thin and discontinuous tracks, due to the reduction in the surface energy of liquid at short length scales. Hence, a large amount of micrometer-scaled spherical splashes are formed around the surface, finally resulting in the balling phenomenon. This is consistent with other cases referring to the balling phenomenon and the melting instability [19,20].

Moreover, an insufficient amount of liquid phase was generated due to a considerably short dwelling time of laser spot at scanning speed 1.2 m/s. The extremely low energy input cannot make the temperature of the irradiated powders higher than that of the melting point 1668 °C of Ti6Al4V alloy. Thus, only sintering necks, formed by means of diffusion, could be found instead of the consolidation of liquid phase. Of course, the produced loosen Ti6Al4V cannot bear excellent mechanical properties.

Corresponding to these top-surface morphologies, the measurement of roughness was carried out. Roughness values Ra were obtained, as shown in Fig. 6. Among the three melted Ti6Al4V parts, the highest smoothness is 2.1 μm corresponds to point 2. This is an almost perfect Ti6Al4V part. While for the other parts, Ra values are relatively much higher because of the existence of pulse craters, convexes and holes arising from cracks and unmelted layers.

3.2. Microstructure and densification

Although selective laser melting using the various parameters within the processing map mentioned above yields a regular top-surface morphology evolution, it is necessary to further observe the microstructure feature on the internal sections of Ti6Al4V samples produced by selective laser melting in order to obtain a reasonable and accurate processing parameter.

Fig. 7 shows typical single Ti6Al4V tracks and cross-sectional micrographs of selective laser melted Ti6Al4V parts corresponding to different processing windows. For point 1 within zone I, a defective microstructure consisting of completely melted zone and cracks was visible. This is consistent with the morphology of single track which broke up at intervals (top in Fig. 7a). At a laser power of 110 W and scanning speed of 0.4 m/s, selective laser melting yields a more homogeneous and almost fully dense microstructure. While a honeycomb-like structure was formed using parameter within zone III. A number of gaps exist on the internal sections of Ti6Al4V samples. Combining the morphology of single track (top in Fig. 7c), it can be found that not only the single track is not continuous but also the part formed by numerous tracks has not a good bonding.

Taking into account the morphology of single tracks, the top-surface of parts and the cross-sectional microstructure of Ti6Al4V parts produced by selective laser melting using different parameters within the processing map, the present results clearly revealed that the cross-sectional microstructure of Ti6Al4V parts is consistent with the top-surface with the same processing parameter and confirmed that the structure and the property of a part produced by SLM technology depend strongly on the property of each single track.

Furthermore, the densification level of selective laser melted Ti6Al4V parts corresponding to different processing windows was investigated. Table 1 depicts the statistics for selective laser melted densities using different parameters. As expected, the density (4.13 g/cm^3) of selective laser melted Ti6Al4V parts using parameters within zone II is so high that it can be comparable to the density (4.30 g/cm^3) of bulk Ti6Al4V alloy.

3.3. Mechanical property

The influence of laser power and laser scanning speed on the microhardness of selective laser melted Ti6Al4V parts is shown in Fig. 8. These processing parameters have an important influence on microhardness, because the microhardness has a direct relationship with the densification level. This is undoubtedly connected with the fact that the densification level corresponds to the resistance to plastic deformation or rupture. In the present paper, the microhardness of the densest part corresponding to zone II (110 W, 0.4 m/s) is 450 HV. This value is much higher than that of thermohydrogen-processed Ti6Al4V part before and after the THP treatment (from 306 to 339 HV) [21] and higher than that of Ti6Al4V part processed by the electron beam welding (from 270 HV to 370 HV) [22]. Comparing these processing methods, it can be considered that the selective laser melting technology has a great potential in fabricating high performance Ti6Al4V part with controlled microstructures and mechanical properties.

4. Conclusions

The processing map for selective laser melting of Ti6Al4V alloy was list systematically, based on the melted single tracks. Then the effect of processing parameters on microstructure and mechanical property of Ti6Al4V parts was investigated in this study. Conclusions could be drawn as follows:

(1) Based on a series of single tracks, three melting mechanism were proposed to later manufacture a real part.

(2) A perfect Ti6Al4V part has been successfully manufactured by selective laser melting using parameters (v = 0.4 m/s, P = 110 W) within zone II, corresponding to continuous melting mechanism.

(3) For the selective laser melted Ti6Al4V part corresponding to continuous melting mechanism, both the smoothness 2.1 μm and the microhardness 450 HV are highest. Moreover, the density 4.13 g/cm^3 is so high that it can be comparable to the density (4.30 g/cm^3) of bulk Ti6Al4V alloy.

References

[1] Fernandez BJ, Damborene J, Ruiz J. Effect of high-temperature surface hardening of metallic materials on their dimensional stability. Mater Des 2002;23:377–83.
[2] Bertol LS, Júnior WK, Silva FP, Aumund-Kopp C. Direct metal laser sintering of Ti–6Al–4V. Mater Des 2010;31:3982–8.
[3] Bandyopadhyay A, Espana F, Balla VK, Bose S, Ohgami Y, Davies NM. Influence of porosity on mechanical properties and in vivo response of Ti6Al4V implants. Acta Biomater 2010;6:1640–8.
[4] Blackburn MJ, Malley DR. Plasma arc melting of titanium alloys. Mater Des 1993;14:19–27.
[5] Abe F, Osakada K, Shiomi M, Uematsu K, Matsumoto M. The manufacturing of hard tools from metallic powders by selective laser melting. J Mater Process Technol 2001;111:210–3.
[6] Das S, Wohlert M, Beaman JJ, Bourell DL. Processing of titanium net shapes by SLS/HIP. Mater Des 1999;20:115–21.
[7] Mumtaz KA, Erasenthiran P, Hopkinson N. High density selective laser melting of Waspaloy®. J Mater Process Technol 2008;195:77–87.
[8] Verhaeghe F, Craeghs T, Heulens J, Pandelaers L. A pragmatic model for selective laser melting with evaporation. Acta mater 2009;57:6006–12.
[9] Brandl E, Heckenberger U, Holzinger V, Buchbinder D. Additive manufactured AlSi10Mg samples using selective laser melting (SLM): microstructure, high cycle fatigue, and fracture behavior. Mater Des 2012;34:159–69.
[10] Hao L, Dadbakhsh S, Seaman O, Felstead M. Selective laser melting of a stainless steel and hydroxyapatite composite for load-bearing implant development. J Mater Process Technol 2009;209:5793–801.
[11] Zhang Y, Xi M, Gao S, Shi L. Characterization of laser direct deposited metallic parts. J Mater Process Technol 2003;142:582–5.
[12] Joo BD, Jang JH, Lee JH, Son YM, Moon YH. Selective laser melting of Fe–Ni–Cr layer on AISI H13 tool steel. Trans Nonferrous Met Soc China 2009;19:921–4.
[13] Gu DD, Hagedorn YC, Meiners W, Wissenbach K, Poprawe R. Selective laser melting of in-situ TiC/Ti5Si3 composites with novel reinforcement architecture and elevated performance. Surf Coat Technol 2011;205:3285–92.

[14] Simchi A. Effect of C and Cu addition on the densification and microstructure of iron powder in direct laser sintering process. Mater Lett 2008;62:2840–3.
[15] Simchi A, Godlinski D. Effect of SiC particles on the laser sintering of Al–7Si–0.3Mg alloy. Scripta Mater 2008;59:199–202.
[16] Zhu HH, Lu L, Fuh JYH, Wu CC. Effect of braze flux on direct laser sintering Cu-based metal powder. Mater Des 2006;27:166–70.
[17] Dewidar MM, Dalgarno KW, Wright CS. Processing conditions and mechanical properties of high-speed steel parts fabricated using direct selective laser sintering. Proc Inst Mech Eng B: J Eng Manuf 2003;217:1651–63.
[18] Gu DD, Shen YF. Influence of phosphorus element on direct laser sintering of multicomponent Cu-based metal powder. Metall Mater Trans B 2006;37:967–77.
[19] Simchi A, Pohl H. Direct laser sintering of iron-graphite powder mixture. Mater Sci Eng A 2004;383:191–200.
[20] Gu DD, Shen YF. Balling phenomena in direct laser sintering of stainless steel powder: metallurgical mechanisms and control methods. Mater Des 2009;30:2903–10.
[21] Yu CY, Yang LX, Shen CC, Luanb B, Perng TP. Corrosion behavior of thermohydrogen processed Ti6Al4V. Scripta Mater 2007;56:1019–22.
[22] Barreda JL, Santamaria F, Azpiroz X, Irisarri AM, Varona JM. Electron beam welded high thickness Ti6Al4V plates using filler metal of similar and different composition to the base plate. Vacuum 2001;62:143–50.